Structural Eng./Earthquake Eng. Vol. 11, No. 2, 103s—114s, July 1994
Japan Society of Civil Engineers (Proc. of JSCE No. 495/I—28)

AN ELASTO-PLASTIC DYNAMIC RESPONSE ANALYSIS OF UNDERGROUND STRUCTURE-SOIL COMPOSITE BASED UPON THE 3-D FINITE ELEMENT METHOD

Yoshitaka OHSHIMA* and
Hiroyuki WATANABE**

Using the three-dimensional finite element method, we have simulated the vibration tests on underground structure-soil composite models. Through these simulations, by modelling the soil and the linkage element of the contacting surface between soil and structure as an elasto-plastic material, it was found that it is possible to simulate the following two phenomena ; the horizontal vibration excites the vertical vibration due to the dilatancy of soil, and the dynamic earth pressures resulting from the horizontal and vertical vibrations act on the structure.

Key Words : *3-dimensional system, soil-structure interaction, separation and sliding, elasto-plastic dynamic analysis, dynamic earth pressure*

1. INTRODUCTION

Recently, application of three-dimensional numerical analysis has increased in number, with the spread of high speed processing computers and their easiness in handling. For example, we know some cases using this method such as the research of seismic response analysis for dams or of flutter analysis for bridges. In the field of the structural engineering, such methodology has been put into practice that idealizes a complicated three-dimensional shaped structure to be assembly of shell elements etc. and then calculates the stresses of the members by applying external force to it statically[1]. Such a three-dimensional analysis reduces the equivocality in modelling and makes a rational and economical design of a structure possible, so that it seems that this analysis will be used more widely in future. In particular, pit-shaped underground structures or underground foundation structures in nuclear power plants which we are going to discuss in this paper are required to have the earthquake resisting of higher level, so that the designing method by the use of three-dimensional stress analysis is desirable and for this purpose, the seismic earth pressure as a main load should be evaluated exactly according to the actual phenomenon.

Since the seismic earth pressure acting on an underground structure generates from the dynamic interaction of ground and structure, the earth pressure especially under strong motion earthquake is largely influenced by the non-linear properties of the ground. So far, with regard to the structures which can be modeled as a two-dimensional problem, the seismic earth pressure for them has been studied and formulated[2] using the 2-dimensional finite element method. However, it is necessary to prepare a new approach to the structures which should be solved through a 3-dimensional procedure. For example, concerning a water intake pit and an underground water reservoir, the seismic earth pressure behavior acting on the exterior walls located parallel to the paper surface (parallel to the direction of the earthquake motion) can not be elucidated qualitatively in the two-dimensional analysis.

For the purpose of studying the seismic earth pressure acting on a 3-dimensional underground structure, the authors carried out first of all sinusoidal excitation experiments on both the free ground model and the underground structure-soil composite model[3]. As a result, it has been found that the horizontal excitation causes the vertical vibration due to the dilatancy of soil, and that the simulation of this phenomenon is possible through the elasto-plastic dynamic analysis based upon the flow theory in which the soil is deemed as a Drucker-Prager material with the Cap. The tests have also revealed that the above excited vertical vibration newly generates the dynamic earth pressure on the exterior walls which are parallel to the excitation direction resulting in the fact that the resultant dynamic earth pressures due to both horizontal and vertical vibrations act on the exterior walls which are perpendicular to the excitation direction.

Although the main purpose of the previous paper[3] was to study the experimental results, this

* Member of JSCE, Civil Engineering Design Dept., MAEDA Corp. (J. CITY, 5-8 Takamatsu, Nerima-ku, Tokyo 179 Japan)
** Member of JSCE, Dr. Eng., Professor, Saitama University

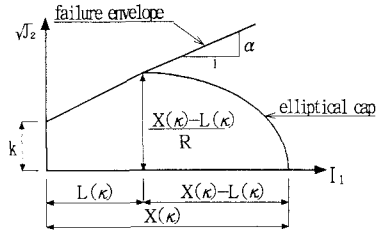

Fig.1 Yield surfaces and parameters of functions

paper aims at proposing a dynamic analysis method considering at the same time both ground material non-linearity and geometrical non-linearity of the contacting surface between the structure and soil. Practically, the underground structure-soil composite as reported in the previous paper is idealized by the 3-dimensional finite element method ; with this model, we perform a simulation of a model vibration test by use of the dynamic response analysis in which the elasto-plastic behavior of the ground as well as separation and sliding at the contacting surface between the underground structure and the soil are taken into consideration. In addition to this, we also perform a simulation presuming that the soil is a linear elastic material. We also try to verify the applicability of our proposed method through the comparison of these analytical results with experimental results.

2. METHOD OF ANALYSIS

(1) Elasto-plastic constitutive relations of soil[4)]

The total strain increment tensor of soil $d\varepsilon_{ij}$ is assumed to be the sum of the elastic strain increment tensor $d\varepsilon^e_{ij}$ and the plastic strain increment tensor $d\varepsilon^p_{ij}$.

$$d\varepsilon_{ij}=d\varepsilon^e_{ij}+d\varepsilon^p_{ij} \quad \cdots\cdots(1)$$

Presuming that the elastic strain increment tensor follows the generalized Hooke's law, and that the plastic stress increment tensor generates in the direction of the outer vector normal to the plastic potential function $g(\sigma_{ij})$, the following equations can be established ;

$$d\varepsilon^e_{ij}=C_{ijkl}d\sigma_{kl} \quad \cdots\cdots(2)$$

$$d\varepsilon^p_{ij}=d\lambda\frac{\partial g}{\partial\sigma_{ij}} \quad \cdots\cdots(3)$$

where C_{ijkl} is the material response function, $d\lambda$ is the positive scalar coefficient being non-zero only when the plastic deformation occurs. In this paper, the associated flow rule is assumed, that is, the plastic potential function coincides with the loading function f. In this study the failure criterion was assumed as the Drucker-Prager one with the Cap. Letting α and k be the material constants of soil, κ be a hardening parameter and R be the elliptic ratio of the Cap, the failure criterion shown in **Fig.1** may be expressed in the following equations of functions h and H.

$$f=\begin{cases} h(I_1,\sqrt{J_2})=\sqrt{J_2}-\alpha I_1-k \\ H(I_1,\sqrt{J_2},k)=\sqrt{J_2}-\frac{1}{R}\{[X(\kappa)-L(\kappa)]^2-[I_1-L(\kappa)]^2\}^{1/2} \end{cases} \quad \cdots\cdots(4)$$

where κ, a function of the hysteresis of the plastic volumetric strain ε^p_{kk}, is assumed to be expressed by the following equation, using the material constants W and D which can be obtained from the isotropic compression test.

$$\kappa=\varepsilon^p_{kk}=W\{1-\exp[-DX(\kappa)]\} \quad \cdots\cdots(5)$$

α and k are determined so that the D-P criterion line and the Mohr-Coulomb criterion line may be circumscribed on the compression meridian.

$$\alpha=\frac{2\sin\varphi}{(3-\sin\varphi)\sqrt{3}} \quad \cdots\cdots(6)$$

$$k=\frac{6c\cos\varphi}{(3-\sin\varphi)\sqrt{3}} \quad \cdots\cdots(7)$$

where c is soil cohesion, and φ is internal friction angle.

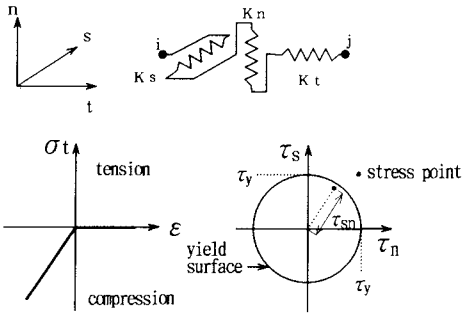

Fig.2 Schematic representation of the linkage element and its constitutive relationships

(2) Elasto-plastic constitutive relations of the linkage element

Linkage elements are placed on the contacting surface between the structure and soil. This element is composed of the spring elements which tie the two nodes having the same coordinates at the opposite sides of the contacting surface, acting as friction springs which intersect orthogonally in the case of sliding on the contact plane, and as an axial spring which is normal to the plane in the case of separation. The linkage element is deemed as having the deformation properties shown in **Fig.2**. Followings are assumed in the element.

a) No transmission of force occurs in the case of separation.

b) In the compression case, the stress and the strain of the axial spring are in linear relationship, and the shear stress and the shear strain of the friction spring is in linear relationship when the absolute value τ_{sn} of the shearing stress is less than the failure stress τ_y, and when it reaches the failure stress, the displacement increases with the value of τ_y kept constant, that is, the relation is an elasto-perfectly plastic character. τ_{sn} and τ_y are given in the following equations.

$$\tau_{sn}=\sqrt{\tau_s^2+\tau_n^2} \quad \cdots\cdots(8)$$

$$\tau_y=\mu\sigma_t+C_h \quad \cdots\cdots(9)$$

where τ_s and τ_n are defined as the shear stresses in the two directions which intersect orthogonnally in the plane, μ and C_h are the friction coefficient and cohesion of the contacting surface, σ_t is the compression stress which acts normally to the contact plane, defined as the sum of the initial and dynamic stresses.

Now τ_y and σ_t in Eq.(9) are deemed respectivey as $\sqrt{J_2}$ and I_1 in Eq.(4) then it can be clearly known that Eq.(9) is same as the function h of Eq.(4). The yield surface of the linkage element with the above relationship can be expressed as a circular cone having a head at the top and a hydraulic pressure axis σ_t in the 3-dimensional stress space. Consequently, for the calculation of the elasto-plastic stress of the linkage element, it is possible to use the same algorism as that for the soil element, which is shown in the following section. However, the next condition must be added that the linkage element produces no plastic volumetric strain ε_{kk}^p, even if the stress reaches the yield surface, because no plastic volumetric change occurs in the linkage element.

(3) Calculation process of the elasto-plastic stress

The calculation process based upon the flow theory is summarized as follows.

First of all, the first invariant of the stress tensor I_1 and the deviatoric stress tensor s_{ij} must be calculated.

$$I_1^e=I_1^n+3Kd\varepsilon_{kk}^{n+1} \quad \cdots\cdots(10)$$

$$s_{ij}^e=s_{ij}^n+2Gde_{ij}^{n+1} \quad \cdots\cdots(11)$$

where $d\varepsilon_{ij}^{n+1}$ is the strain increment tensor at the step of $n\sim n+1$, the superscript e means elasticity. Generally, the bulk modulus K and shear modulus G are respectively the functions of the first invariant of the stress tensor, the second invariant of deviatoric stress tensor $J_2=1/2s_{ij}s_{ij}$ and the plastic strain tensor ε_{ij}^p.

$$K=K[I_1^n,\ (\varepsilon_{ij}^p)^n] \quad \cdots\cdots(12)$$

$$G=G[\sqrt{J_2^n},\ (\varepsilon_{ij}^p)^n] \quad \cdots\cdots(13)$$

When Eq.(10) and Eq.(11) are checked for the yield surfaces of Eq.(4), if $f\leq 0$, the material behavior is elastic, and its stress at the $n+1$ step is given as follows ;

$$I_1^{n+1}=I_1^e \quad \cdots\cdots(14)$$

$$s_{ij}^{n+1}=s_{ij}^e \quad \cdots\cdots(15)$$

If $f>0$ and $h>0$, I_1 at the $n+1$ step is calculated by the following equations, where the D-P criterion of Eq.(4) is expressed as $h(I_1,\ \sqrt{J_2})=\sqrt{J_2}-Q(I_1)$.

$$I_1^{n+1}=I_1^e-3Kd\varepsilon_{kk}^p \quad \cdots\cdots(16)$$

$$d\varepsilon_{kk}^p=-3\left[\frac{\sqrt{J_2^e}-Q(I_1^e)}{9K\left(\frac{\partial Q}{\partial I_1}\right)^2+G}\right]\frac{\partial Q}{\partial I_1} \quad \cdots\cdots(17)$$

If $I_1^{n+1}>L(\kappa^n)$, I_1 at the $n+1$ step is obtained by the following equations instead of Eq.(16).

$$I_1^{n+1}=\frac{bI_1^e+3Kl^n}{b+3K} \quad \cdots\cdots(18)$$

$$b=\left.\frac{\partial l}{\partial \varepsilon_{kk}^p}\right|_{l^n} \quad \cdots\cdots(19)$$

$$l^n=L(\kappa^n) \quad \cdots\cdots(20)$$

If I_1 is larger than the Cap, a trial value dl is assumed in order to compute $l^t=l^n+dl$ till the following equation becomes effective with a sufficiently small admissible value C_a, where the Cap is expressed as $H(I_1,\ \sqrt{J_2},\ \kappa)=\sqrt{J_2}-F(I_1,\ \kappa)$.

).

$$\left|\sqrt{J_2^e}-\sqrt{J_2^t}-\frac{Gd\varepsilon_{kk}^p}{3a}\right|<C_a \quad \cdots\cdots(21)$$

$$a=-\left.\frac{\partial F}{\partial I_1}\right|_{I_1^t,I^t} \quad \cdots\cdots(22)$$

I_1^t, J_2^t, satisfying the above equations, are the invariants of the stress at the $n+1$ step, the stress tensor σ_{ij}^{n+1} is expressed as follows ;

$$s_{ij}^{n+1}=\frac{\sqrt{J_2^{n+1}}}{\sqrt{J_2^e}}s_{ij}^e \quad \cdots\cdots(23)$$

$$\sigma_{ij}^{n+1}=s_{ij}^{n+1}+\frac{I_1^{n+1}}{3}\delta_{ij} \quad \cdots\cdots(24)$$

where δ_{ij} is the Kronecker delta.

(4) Initial stress analysis

In order to solve elasto-plastic dynamic problems based upon the flow theory, it is necessary to pursue the successive stress path and to check whether it reaches the yield surface. For this purpose, the initial stress of ground elements and linkage elements due to the gravity load must be obtained. The most widely used method to compute the initial stress of such a composite model would be a gravity load analysis, in which

the overall system is modelled under the boundary condition that the lateral surfaces can move only in the gravity direction and the bottom of the composite model is fixed in all directions. However, in the case of structure-soil composite discussed in this paper, the above gravity load analysis will involve a risk that the magnitude of stiffness of the linkage element may influence the displacement distribution of structure-soil contacting surfaces ; consequently, not only the initial stress of linkage elements but also that of ground elements are subjected to this influence. Therefore, we introduce the following procedure so that the stiffness of linkage elements may not influence the analytical results. All of the nodes in the composite model are made free in the gravity direction only, and the nodes of the bottom of the structure and the ground nodes contacting with them are displacement-restricted so that they may respectively undergo the same amount of settlement. The friction springs of the linkage element are set as zero, and no shearing forces are supposed to act on the contacting surfaces in the initial stress condition. By the elastic analysis due to the gravity load for such a structure-soil composite model, we obtained the initial stresses of ground elements and linkage elements of the bottom of the structure. Since it is impossible to calculate the initial stress of lateral linkage elements from this analysis, the earth pressure $\{q\}$ similar to hydrostatic distribution is assumed to act on the walls of the structure, and the equivalent nodal force $\{F\}$ obtained by the equation below is used as the initial stress.

$$\{F\}=\int [N]^T\{q\}\,dA \cdots\cdots (25)$$

where $[N]$ is the matrix of shape function for the element under earth pressure. Supposing the ground as a semi-infinite elastic body, the lateral pressure coefficient of earth pressure load is calculated from the ratio of horizontal/vertical ground stress. When ν denotes the Poisson's ratio, the lateral pressure coefficient K_s is expressed in the following equation.

$$K_s=\frac{\sigma_x}{\sigma_z}=\frac{\nu}{1-\nu} \cdots\cdots (26)$$

(5) Response analysis

The step by step integration method has been used for the response analysis with $\beta=1/4$ of the Newmark's β scheme, and the Reyleigh type damping matrix shown as follows,

$$[c]=1.4h\omega_1[m]+0.6\frac{h}{\omega_1}[k] \cdots\cdots (27)$$

where $[m]$ and $[k]$ denote respectively the element mass and stiffness matrixes, ω_1 the primary natural angular frequency. h denotes the damping constant, being defined for the elastic material as the value including both internal and hysteresis dampings, but for the elasto-plastic material, the internal damping only is considered here because the elasto-plastic analysis based upon the flow theory itself includes the hysteresis damping caused by plastic strain. The initial stress method[5] was used for analyzing the non-linear behavior of material.

3. NUMERICAL MODELS AND MATERIAL CONSTANTS

The numerical simulations were carried out on the vibration tests in the previous work of Ref.3) in this paper. In order to facilitate the understanding of numerical simulations, the model vibration tests are outlined as follows.

The tests were performed for both the free ground model and the underground structure-soil composite model. Air-dried Gifu sand was utilized as the material of ground model. The sand was dropped into a shear testing soil container on a shaking table, and compacted under the sinusoidal excitation of 300 gal, 25 Hz feeding with supplementary sand to make up for the settlement to prepare the 50 cm thick ground model. The structure model (outer dimensions : 30 cm long, 21 cm wide, 15 cm high) was made of acrylic resin plates, the surface of which was uniformly coated with the same sand as the ground material to increase the coarseness of the surface of the structure. The experiments were the vibration tests to obtain the resonance curves with horizontal sinusoidal excitations with maximum accelerations of 50 gal, 100 gal and 200 gal, and the frequency was changed from 10 Hz to 60 Hz at each of them. The shear testing soil container used for this experiment is composed of 16 rectangular frames of light weight shaped steel members which are piled up interposing ball bearings between each of them and is rubbered on its inner and outer surfaces. The inner dimensions of it are 1.2 m long, 0.8 m wide, 0.96 m deep. The natural frequency of the container itself was 1.6 Hz.

(1) Numerical models

Since the free ground model in the tests could be assumed to be uniform in its physical properties through over the horizontal plane, a 50 cm high soil column was modelled as an assembly of isoparametric elements of hexahedrons with 8 nodes. The two models shown in **Fig.3** were prepared to verify the influence of idealization. Model-1 is a free ground model which corresponds to the idealization for the structure-soil composite. The nodes on the sides of the model which have the same Z coordinates were displacement-restricted

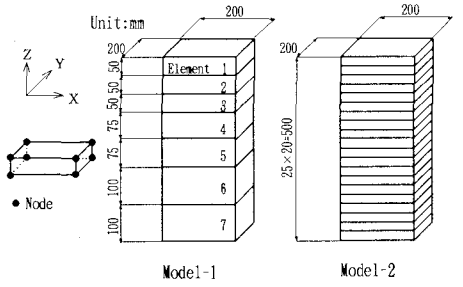

Fig.3 Finite element idealizations of free ground in numerical model

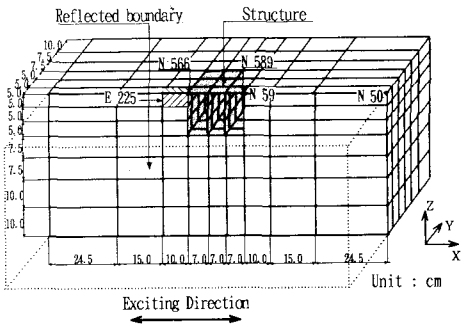

Fig.4 Finite element idealization of soil-structure composite in numerical model

so that they may undergo the same displacements in X, Y, Z directions. The bottom of the numerical model was assumed as a fixed boundary. The authors have already reported that the horizontal excitation produces the vertical vibration due to the dilatancy of soil. Thus, under the above boundary conditions, it is possible to simulate the above mentioned phenomena in the experiment based upon the finite element method.

Fig.4 shows a finite element idealization for the soil-structure composite model. The exterior walls of the structure were modelled by outer dimensions, and the partitions were by the neutral planes with 4-node shell elements. The ground was modelled as an assembly of isoparametric elements of hexahedrons with 8-nodes, providing the linkage elements at the contact portions between the structure and soil. As for the soil-structure composite, only a half of its whole was idealized in the direction normal to the excitation, considering the symmetry in both geometry and vibration load applying the symmetric boundary conditions to the cut section. When simulating the experiments, the bottom of the model was the fixed boundary, and for the sides, as shown in **Fig.5**, two kinds of boundary conditions were provided to review the influence of the stiffness of the shear testing soil container. **Fig.5** illustrates the same composite

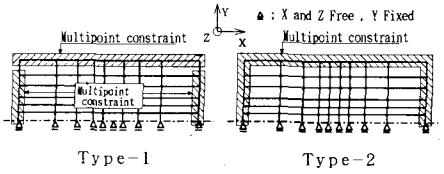

Fig.5 Boundary conditions of soil-structure composite in numerical model

Table 1 Numerical cases of soil-structure composite model

	Ground Model		Boundary Condition	
	Elastic	Elasto-Plastic	Type-1	Type-2
CASE-E1	○		○	
CASE-E2	○			○
CASE-P1		○	○	
CASE-P2		○		○

system as that shown in **Fig.4**, but the one viewed from the positive direction of Z coordinate. Type-2 shows that all the nodes having the same Z coordinate in all side boundaries except for symmetric boundary are allowed to have the same displacements only in X and Z directions, but Type-1 shows that all the nodes having the same Z coordinate only at the side parallel to the exciting direction, independently of the sides perpendicular to it, are allowed to have the same displacements in X, Y and Z directions respectively. That is, in the case of Type-1, the shear testing soil container has no stiffness against the Y-directional deformation at the side parallel to the exciting direction, but in the case of Type-2, infinite stiffness. Actually, as the stiffness of light weight shaped steel rectangular frames constrains the Y-directional deformation, the experimental results should exist within a range between the numerical results of the boundary conditions of Type-1 and Type-2.

(2) Cases of analyses

For the free ground, the elasto-plastic analyses were performed on the FEM models of **Fig.3**. For the soil-structure composite, four cases shown in **Table 1** were performed, and in these cases the separation and sliding of the linkage elements at the contacting surfaces were taken into consideration. The duration of sinusoidal excitation was 0.2 second with a time interval of 0.0005 second and the iterative calculation was continued till the difference between the new displacements and the previous displacements of every node became less than 1×10^{-6} cm . This convergence value was sufficiently small in comparison with the maximum response displacement 0.024 cm at the ground surface of Model-1 for instance.

(3) Material properties

The material properties used for the analyses are shown in **Table 2**. The ground shear modulus G is

Table 2 Material properties in numerical model

1 kgf/cm² = 98 kPa

Properties			Soil	Structure	Linkage
Shear modulus	G	kgf/cm²	*1)	2.7×10^4	—
Poisson's ratio	ν	—	0.25	0.2	—
Unit weight	γ	gf/cm³	1.369	1.19	—
Cohesion	c	kgf/cm²	0.01	—	0.01
Friction angle	ϕ	deg.	27.5	—	27.5
Damping constant	h	%	*2)	5.0	0.0
Parameter of hardening function	D	$(\text{kgf/cm}^2)^{-1}$	0.0121	—	—
	W	—	0.092	—	—
Elliptical ratio	R	—	3.0	—	—
Spring constant	k	kgf/cm³	—	—	100

*1) Initial stress analysis : 5.0 kgf/cm²
Dynamic analysis : $G=\beta\times G_0$ $G_0=700[(2.17-e)^2/(1+e)](\sigma'_m)^{0.321}$
β : modificating factor
*2) Elastic case 11.0% , Elasto-plastic case 1.0%

given as a product of G_0, as a function both of void ratio e and of confining pressure σ'_m, and a modificating factor β.

$$G=\beta\times G_0 \quad \cdots\cdots(28)$$

$$\beta=\left(\frac{f_1}{f_0}\right)^2 \quad \cdots\cdots(29)$$

$$G_0=700\frac{(2.17-e)^2}{(1+e)}(\sigma'_m)^{0.321} \quad \cdots\cdots(30)$$

where f_0 is the primary natural frequency obtained from the eigen value analysis with G_0, and f_1 is the resonance frequency obtained from the acceleration resonance curve of the experiment. Eq.(28) means that the ground properties are modified to produce a resonance state in the numerical simulation with the sinusoidal excitation of frequency f_1.

With regard to the parameters for soil, W and D were determined referring to the isotropic compression test[6] of a standard sand which is similar to Gifu sand. As for R, 3.0 was adopted so that the ratio of vertical acceleration to horizontal one becomes largest in this study. R in the range of 2.0 ~ 4.33 has been used for the analyses in the forgoing studies[4),7)]. In the cases that soil was assumed as a linear elastic material in our study, the damping constant was assessed to be about 11% referring to the forgoing numerical simulation[8] based upon the equivalent linear analysis, and in the cases of an elasto-plastic material, the damping constant was determined to be 1% because in this case only the internal damping constant was needed and in accordance with the results of forgoing study[9] that the damping constant in micro strain level is 1 to 2%. The structure was modeled to be a linear elastic material with the damping constant and the Poisson's ratio of 5% and 0.2 respectively which are generally used for the concrete structures. Other material constants concerning the structure and soil models were determined referring to Ref.10).

The cohesion and internal friction angle of the linkage element were supposed to be same as those of soil, and damping constant to be 0%. Therefore, no damping arises as far as the stress in the linkage element is kept in the range of elasticity, but the hysteresis damping due to the plastic strain comes out when it reaches the yield surface. The larger stiffness of linkage element is more desirable for the sake of emphasizing that the ground and the structure elements do not interpose to each other. However, with the excessively large stiffness, errors may occur in the numerical analysis, and the number of iterations up to the convergence may become extremely large. To avoid these drawbacks, we have reviewed the influence of the spring constant of the linkage element on the response, comparing the primary eigenvectors for Node 589 at the top of the structure and Node 59 at the surface of the ground shown in **Fig.4** with those of a composite model without linkage element. The results are shown in **Table 3**. Even if the spring constant was changed from 10 kg/cm³ to 1 000 kg/cm³, a negligibly small change occurred in the natural frequency, but a considerable effect was brought to the eigenvector in Z direction. Considering the result of review and the number of iterations up to convergence, both the compression and shearing spring constants were determined 100 kg/cm³. The number of iterations up to convergence which were made with the initial stress method[5] for the elasto-plastic analysis did not depend on the non-linear calculation for the soil plastic stress, but on the spring constants of the linkage element.

Table 3 Relationships between natural frequency, proper vector and magnitude of spring constants of linkage element

1 kg/cm³ = 98 kPa/cm

Spring Constant (kg/cm³)		Natural Frequency(Hz)	Horizontal Component of Proper Vector		Vertical Component of Proper Vector	
K t	K s n		Node-589	Node-59	Node-589	Node-59
10	10	52.56	2.62	2.53	0.0795	-0.0570
100	100	52.72	-2.48	-2.46	0.0437	0.0505
1000	1000	52.76	-2.45	-2.45	0.0499	0.0500
∞	∞	52.76	-2.45	-2.45	0.0499	0.0499

4. NUMERICAL RESULTS

(1) Numerical results of the free ground

We carried out vibration tests to obtain resonance curves with horizontal sinusoidal excitations on the free ground model, and we found out that when the ground is excited only horizontally, the volume change of soil produces the vertical vibration, and its frequency is just 2 times larger than the horizontal one. Then, in the following, we performed the numerical simulation of the test of the sinusoidal excitation under 200 gal in the amplitude and 35 Hz in the frequency with the FEM model shown in **Fig.3** in order to conduct the comparison between the measured accelerations

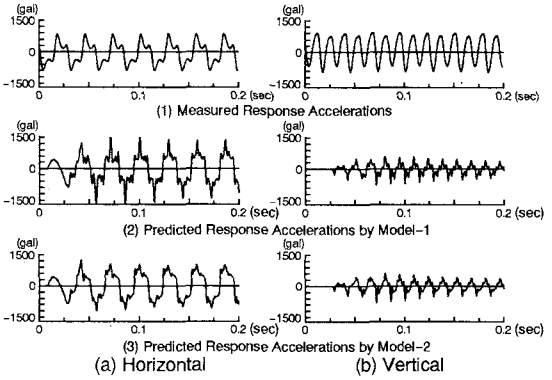

Fig.6 Comparison of measured response accelerations and predicted ones

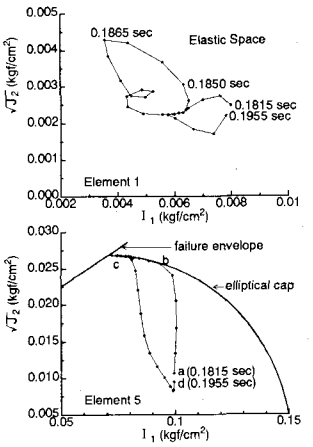

Fig.7 Predicted stress paths of model-1 in meridian planes

and the predicted accelerations, and also to study the idealization effect on the predicted accelerations and the relationship between stress and strain of soil.

a) Comparison of measured response accelerations and predicted ones

Fig.6 shows the time histories of measured accelerations as well as predicted ones of Model-1 and Model-2 at the ground surface. The measured ones are the accelerograms during 0.2 second extracted from the steady state recorded data, but the predicted ones include transient state. Even though the calculation was performed under such simple assumption that the ground was of the Drucker-Prager material to be easily handled in numerical calculation and in the elastic range the shear modulus obtained from Eq.(28) was adopted, the predicted acceleration reproduced well the characteristics of the measured one, specially in the points that the vertical vibration is 2 times larger in frequency than the horizontal one and the shape of horizontal acceleration was similar to that of measured one. Furthermore, the phase relationship between horizontal and vertical accelerations was same as the measured one, that is ; the vertical acceleration has the negative peak when the horizontal one reaches both positive and negative peaks, and has the positive peak when the horizontal one crosses zero. Here, let us study this phase relationship in terms of displacement. When the acceleration is converted through integration into the displacement, the positive-negative relationship is inversed. The vertical displacement has the positive peak whenever the horizontal displacement reaches maximum, so that this means a volume swelling. On the other hand, the vertical displacement has the negative peak when the horizontal displacement crosses zero, so that this means a volume shrinkage.

This phenomenon is explained as follows in the numerical analysis. **Fig.7** shows stress pathes of Element 1 and Element 5 on the meridian plane in the 3-dimensional principal stress space from 0.1815 second to 0.1955 which corresponds to about one period of the vertical vibration. The stress of Element 1 does not reach the yield surface, but draws a complicated path under the influence of plasticization in lower layers. The stress path of Element 5 is a typical example of plasticized element, and all the other plasticized elements have plastic strain on the Cap like this. In path from **a** to **c**, $\sqrt{J_2}$ increases and I_1 decreases, in other words, this means that the absolute value of shear stress goes up towards the maximum value and the compression stress goes down towards the minimum value. This means volume swelling. In the case of the path from **c** to **d**, $\sqrt{J_2}$ decreases with increasing I_1, this means that the shear stress goes down towards zero, and the compression stress goes up towards the maximum, in other words, volume shrinkage. The repetition of this phenomenon results in the vertical vibration. However, because in the stress path from **b** to **c** the plastic volume strain occurs in the direction in which I_1 increases, the plastic volume strain is accumulated after every cycle. Consequently, the settlement continues during vibration. At the experiment, however, it seemed that the settlement ceased. The way to mitigate the gap in the displacement as well as the more accurate prediction of vertical acceleration should be studied further in the future.

The idealization influence on the response appears as pulses at the top of the horizontal acceleration in the Model-1 as shown in **Fig.6**. This portion in the numerical analysis shows the response acceleration at the moment when the stress in soil element reaches the Cap. It is generated by a rapid increase of the supplemental

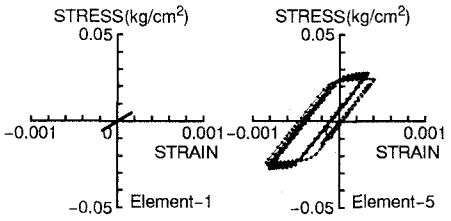

Fig.8 Hysteresis loop of τ_{xz}-γ_{xz} in Model-1

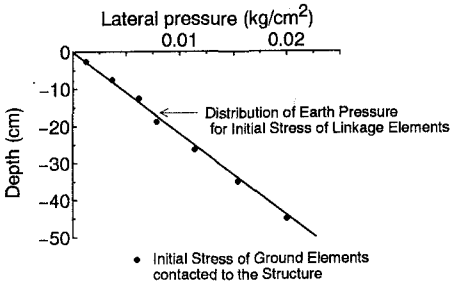

Fig.9 Comparison of distribution of earth pressure for initial stress of linkage elements with initial stress of ground elements

external force in the initial stress method which is calculated as a difference between the elastic stress calculated from Eq.(10) and Eq.(11) and the plastic stress from Eq.(24). In Model-2 above pulses decrease. The reason why no excessive increase in the acceleration occurs at the peak of Model-2 seems to be attributable to the fact that as the number of elements becomes larger, there occurs the difference of time the stress reaching the Cap among the elements so that the external force does not accumulate excessively.

b) Hysteresis loop

Fig.8 shows the relationships between the shear stress (τ_{xz}) and the shear strain (γ_{xz}) for Element 1 and Element 5 of Model-1. We know as well that the stress of Element 1 does not reach the yield surface. Element 5 gives a typical shear stress-shear strain relationship in the case of plasticization, and the supposed soil material properties draw a hysteresis loop of elastic work-hardening plastic strain under the cyclic loading. The damping of soil is expressed with 1% of the inputted internal damping and with the dissipation of energy due to the hysteresis loop. The hysteresis loop of Model-2 was approximately similar in form to that of Model-1, and no influence by the idealization on the hysteretic damping was obtained.

(2) Analysis of the soil-structure composite

From the experiment of the soil-structure composite, it was observed that the dynamic earth pressure which is caused by the vertical vibration due to the dilatancy of soil, acts on the exterior walls parallel to the exciting direction, and that one caused by both the vertical and horizontal vibrations acts on the exterior walls perpendicular to the exciting direction. As a feature in the above, the dynamic earth pressure caused by the horizontal vibration has the same frequency as the exciting acceleration, but the one caused by the vertical vibration has the frequency 2 times larger than the exciting acceleration. Then, we perform the numerical simulations of the test of the sinusoidal excitation under 200 gal in the amplitude and 37 Hz in the frequency with the FEM model shown in **Fig.4** in order to compare the measured results with the predicted ones. Since there is no paper about the elasto-plastic dynamic response based upon the flow theory of such a composite model as ours to which we can make reference, we intend to clarify the characteristics of our results by making use of the comparison of them with the results of the dynamic analysis carried out under the assumption that soil is a linear elastic material.

a) Result of the initial stress analysis

This study, as discussed in Chapter 2, has a requirement that the stiffness of the linkage element does not influence on the analytical results. Considering the requirement, the initial stresses of the ground and the linkage elements at the bottom of the structure were calculated from the 3-D FEM model with gravity load, and the initial stresses of the linkage elements at the lateral sides of the structure were are determined from the static earth pressure distribution. **Fig.9** shows the horizontal components of the stress in a soil element thus calculated superimposing the static earth pressure distribution. From this figure, it is known that the both initial stress of soil and linkage elements agree satisfactorily with each other, and this means the system as a whole is of good consistency. The initial stress of the linkege elements at the bottom of the structure was 10.455 g/cm², and this means that the reaction earth pressure is uniformly distributed with the value that the weight of the structure is averaged by the bottom area.

b) Vibration characteristics of the structure and ground

The predicted response accelerations of the structure and ground are given in **Fig.10**. The response acceleration of Node 50 on the side boundary indicates that no vertical vibration occurs in CASE-E 1. From this, we know that the present boundary condition constrains rocking vibration for the whole of the soil-structure composite system. In CASE-P 1, the horizontal and the vertical vibrations are similar to those of the free

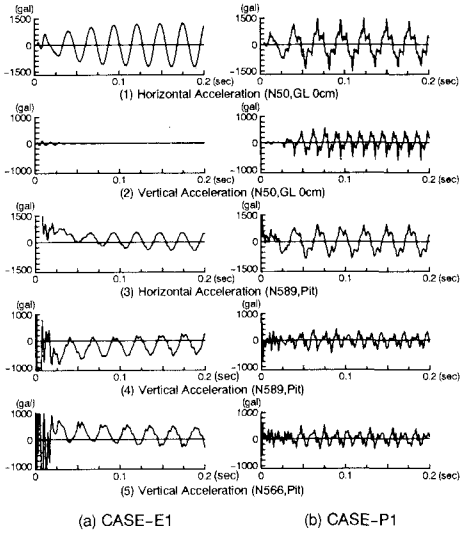

Fig.10 Comparison of predicted accelerations between CASE-E 1 and CASE-P 1

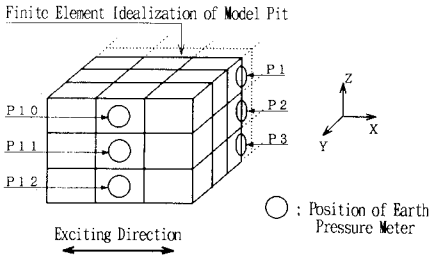

Fig.11 Finite element idealization of model pit and location of earth pressure meter used in experiment

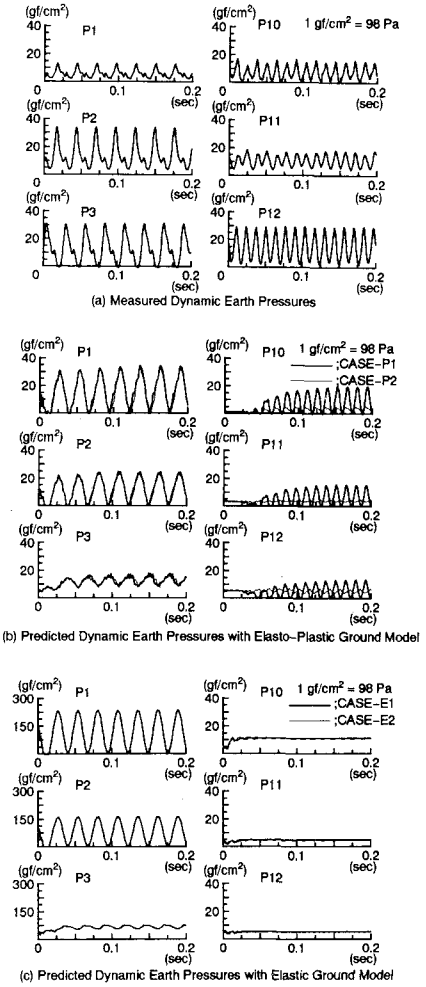

Fig.12 Comparison of measured dynamic earth pressures with predicted ones

ground as shown in **Fig.6**, but comparing calculated values with the measured ones in amplitude, the predicted ones are about 1.5 times larger in the horizontal vibration, and about 0.5 times larger in the vertical vibration than those of measured. As mentioned in the free ground analyses, these differences seem to be attributed to the rough idealization in the depth direction and to the simplicity of the assessment of the soil properties. Focusing the predicted response accelerations of the structure, the vertical vibrations are completely different to each other in both cases. By comparing the response accelerations of the Node 589 and Node 566 which are located at the both sides of the structure, it is known that the structure of CASE-E 1 made rocking vibration. Although accelerations of CASE-P 1 contain high frequency components, the vertical vibrations which are 2 times larger in frequency than the horizontal one occure without phase inversion in the both nodes. This phenomenon agrees with the experiment results. The same results were obtained for the boundary conditions of Type-2.

c) Study on dynamic earth pressure

The dynamic earth pressure was assessed as the nodal force of the linkage element. However, since the number of shell elements used for modelling the structure was decreased so as to decrease the total freedoms of composite model, there is no node of the FEM model that just coincides with the location of the earth pressure meter used for the experiment. **Fig.11** shows the location of the earth pressure meters on the structure idealization. Thus, the predicted dynamic earth pressure of P 1, P 2 and P 3 on the wall perpendicular to the exciting direction were calculated from the mean of upper and lower nodal forces, and those of P 10, P 11 and P 12 on the wall parallel to the exciting direction were from the mean of 4 nodal forces which surround an earth pressure meter. **Fig.12** shows the measured dynamic earth pressures and pre-

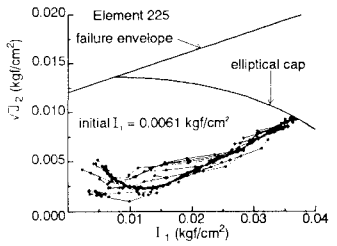

Fig.13 Predicted stress path of CASE-P 1 in Meridian Plane

dicted ones. In Ref.3), the measured ones are shown as a ratio to the static earth pressure, but in this paper, they are indicated as the measured values directly to make the comparison with the predicted ones easily.

The measured dynamic earth pressure on the wall perpendicular to the exciting direction was a resultant wave being superposed by the following two kinds of dynamic earth pressure, that is, one due to the horizontal vibration of the same frequency as the sinusoidal excitation and the other due to the vertical vibration which is 2 times larger in frequency than the former one. The phase of P 3 was opposite against those of P 1 and P 2. In the elasto-plastic analysis, the predicted dynamic earth pressures coincide perfectly with the measured ones with respect to the phase of time history, and the agreement in the magnitude is fairly good. The difference of side boundary condition parallel to the exciting direction exerts almost no influence on the predicted dynamic earth pressure. With regard to the wave form of the predicted dynamic earth pressure, the part due to the horizontal vibration only dominates, and the part due to the vertical vibration cannot be found. The reasons are considered as follows. Firstly, the predicted response acceleration is almost 1.5 times as large as the measured one in the horizontal direction and about 0.5 times as large as the measured one in the vertical direction, so that the predicted dynamic earth pressure resulting from the vertical vibration is relatively smaller than that from the horizontal vibration. Secondly, the side boundary condition perpendicular to the exciting direction of the soil-structure composite model may influence on the predicted dynamic earth pressure. About this issue, we will discuss further later.

With an assumption that the soil was a linear elastic material, the predicted dynamic earth pressures agreed with the measured ones in the phase of time history, and the difference of the side boundary condition parallel to the exciting direction did not influence on the analytical results. The above facts are same as the case of elasto-plastic material, however, the predicted dynamic earth pressures were assessed considerably larger than the measured one. Let us consider the reason of above results by means of examining the stress path in the Element 225 which adjoints P 1 whose predicted value was about 15 times larger than the measured one. **Fig.13** shows the predicted stress path in the case of elasto-plastic material. The stress change in I_1 direction is more remarkable than that in $\sqrt{J_2}$ direction, and strain hardening occurs on the Cap. In other words, because of the plasticization, the predicted dynamic earth pressure was not excessively assessed in the elasto-plastic analysis, while with the assumption of the linear elastic material, because of having no regard to the process of strain hardening in the compression stress, the predicted one was overestimated.

As for the measured dynamic earth pressures on the wall parallel to the exciting direction, the dynamic earth pressures of the frequency 2 times larger than those of the sinusoidal excitation were observed and all the phases of them in any level of depth agreed to each other in the experiments. In the case of the elasto-plastic analysis, the difference of side boundary condition of the composite significantly influenced on the predicted dynamic earth pressures on the wall parallel to the exciting direction. In CASE-P 2 in which the displacement in Y direction of the side boundary parallel to the exciting direction was constrained, the frequency of the predicted dynamic earth pressure coincided with the measured one, however, the phase of the response time history at P 10 reversed against those of P 11 and P 12. The amplitude of predicted dynamic earth pressure was smaller than the measured one, even if the difference between the measured acceleration and predicted one was taken into consideration. On the other hand, in CASE-P 1, in which the Y-directional displacement of the side boundary parallel to the exciting direction was made free, the phase of the predicted dynamic earth pressure agreed with the measured one and yet differing from CASE-P 2, the amplitude of the predicted value is larger than the measured one when the difference between the measured and predicted accelerations was taken account of. Since the stiffness of light weight shaped steel rectangular frames constrains the Y-directional deformation of the shear testing soil container, the experimental results should lie at a value between the predicted values of CASE-P 1 and CASE-P 2. From above studies we found that the width in Y-direction of the shear testing soil container changes due to the volume change of soil as shown in **Fig.14**, so that if this vibration mode is not taken into account, the predicted dynamic earth pressure due to the

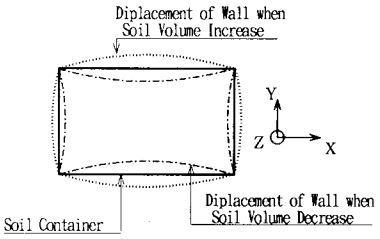

Fig.14 Schematic of displacements of soil container due to volume change of soil

vertical vibration should be underestimated, as well as the phase of the predicted earth pressure should be different from that of measured one. Since the opposite sides of the shear testing soil container perpendicular to the exciting direction were constrained under the same deformation in both in CASE-P 1 and CASE-P 2, we could not express the vibration mode of the soil container in X-direction as shown in **Fig.14**. Therefore, the predicted dynamic earth pressures at the positions of P 1, P 2 and P 3 shown in **Fig.11** resulting from the vertical vibration in the elasto-plastic analysis were also underestimated.

Concerning the case of analysis in which the soil was deemed as the linear elastic material, the difference of side boundary condition did not exert any effect on the results, and yet no vertical vibration occured, so that no dynamic earth pressure of 2 times larger in frequency than the horizontal one occured. Such statement as the above may give an impression as if no predicted dynamic earth pressure was produced on the wall parallel to the direction of excitation, but in the calculated results, due to the horizontal vibration of ground near the wall, the shell elements were subjected to the normal stresses of soil elements which had the same frequency as that of the horizontal vibration. The nodal forces of the two nodes which are symmetrical about the center line of the earth pressure meter were of same amplitude, but opposite in phase so that the mean of the nodal forces defined as the predicted dynamic earth pressure was estimated to be zero because the above nodal forces canceled to each other. But, even if every nodal force was assumed as the predicted dynamic earth pressure directly, its frequency was same as that of the horizontal vibration and this is different from the experimental result.

5. CONCLUSIONS

The model vibration tests on the dynamic interaction between the structure and soil were simulated with the 3-dimensional finite element procedure. The ground was modelled as the Drucker-Prager material with the Cap, and the contacting surface between the structure and soil was modelled with the linkage elements in order to take the separation and sliding into consideration. The analysis was carried out for the case of the resonance state under the sinusoidal excitation of 200 gal in the amplitude. Through the analyses, the followings are obtained;

(1) From the consideration of the phases in time histories of both horizontal and vertical accelerations of the free ground vibration tests, it was found that the volume swelling or shrinkage of the ground occurs when the horizontal displacement increases or decreases.

(2) In the numerical analysis, such phenomenon mentioned above could be explained well by the stress path producing plastic strain on the Cap. Consequently, with the elasto-plastic analysis based on the flow theory used in this study, it was possible to explain the mechanism of vertical vibration due to the dilatancy of soil.

(3) When the soil was assumed as linear elastic material, it was impossible to simulate the excitement of the vertical vibration resulting from the horizontal one. The structure was subject to rocking vibration, and this result was different from the experimental one. On the assumption of elasto-plastic material, the vertical vibration due to the horizontal excitation occured and the structure vibrated horizontally and vertically in almost the same phase as the ground. This phenomenon agreed with the experiment result.

(4) The measured dynamic earth pressures due to the horizontal vibration were phase-inversed in a vertical line on the outside wall. This phenomenon was also confirmed in the analysis regardless of the modelling of soil. When the soil is assumed as elasto-plastic material, the predicted dynamic earth pressure was approximately same as the measured one, but in the case of linear elastic material, that was about 15 times larger than the measured one. In the case of elasto-plastic analysis, overestimate of the predicted dynamic earth pressure was constrained by considering the strain hardening of the soil in the compression stress state.

(5) In the elasto-plastic analysis, the dynamic earth pressure resulting from the vertical vibration of 2 times larger in frequency than the sinusoidal excitation occured on the outside wall parallel to the exciting direction. It was known from the comparison of analytical results for the different boundary conditions that the stiffness of the shear testing soil container gave a significant effect on the dynamic earth pressure due to the vertical vibration. In other words, the shear testing soil

container presented a behavior that the distance of the opposite sides increases or decreases according to the volume change of soil. In the case of neglecting this behavior, the predicted dynamic earth pressure was underestimated.

(6) In relation with (5) above, if a real structure in the semi-infinite ground is considered, the structure and the adjacent ground are supported with the stiffness of the surrounding ground. Therefore, as measured by the experiment, the dynamic earth pressure due to the vertical vibration can be assumed to act on the structure.

(7) If the stiffness of the shear testing soil container was considered in the numerical analysis, the quantitative assessment of dynamic earth pressure was possible by use of the elasto-plastic analysis based on the flow theory used in this study.

As mentioned above, the analytical results were studied with the comparison of the results in the cases of modeling the ground as both elasto-plastic and linear elastic to each other as well as the comparison of them with the vibration test results. From these, we may say that with the elasto-plastic analysis based on the flow theory it is possible for us to evaluate quantitatively the dynamic interaction between the structure and soil which indicates a non-linear behavior under strong earthquake motions. In the case of assuming the soil as linear elastic material, the quantitative evaluation of the horizonal response acceleration is possible, but the dynamic earth pressure tends to be overestimated. It goes without saying that it is impossible to analyze the phenomenon resulting from the dilatancy of soil.

At the end of this paper, we would like to express our gratitude to Mr. Ikuhisa Kato, Maeda Co. Ltd. for his assistance in the numerical analysis, and Dr. Hideji Kawakami, professor of Saitama University for his precious advice.

REFERENCES

1) JCI : A guideline for the application of FEM analysis to concrete structures, 1989.3. (in Japanese)
2) Hiroyuki Watanabe : A theory on dynamic earth pressures acting on underground conduit during earthquake, Proc. of JSCE, No.432/I-16, pp.185～194, 1991.7. (in Japanese)
3) Yoshitaka Ohshima, Hiroyuki Watanabe : An experimental study on elasto-plastic dynamic interaction of 3-D underground structure and soil, Proc. of JSCE, No.489/I-27, pp.261～268, 1994.4. (in Japanese)
4) W.F. Chen, G.Y. Baladi : SOIL PLASTICITY, Elsevier, 1985.
5) O.C. Zienkiewics, S.Valliappan, I.P. King : Elasto-Plastic solutions of engineering problems 'initial stress', finite element approach, Int. J. for Numerical Methods in Engineering, Vol.1, pp.75～100, 1969.
6) Masami Yasunaka, Tadatsugu Tanaka, Ryoki Nakano et al. : Experimental study on the seismic behavior of earth dams by the shaking table tests, Bulletin of the National Research Ins. of Agri. Eng., Vol.27, 1988.2. (in Japanese)
7) D.S. Desai, H.J. Siriwardane : Constitutive laws for engineering materials with emphasis on geologic materials, Prentice Hall, 1984.
8) Hiroyuki Watanabe, Toshio Suehiro : A method to estimate the normal dynamic earth pressure acting horizontally on side walls of underground conduit, Proc. of JSCE, No.432/I-16, pp.165～174, 1991.7. (in Japanese)
9) JSCE : Dynamic analysis and aseismatic design, Vol.1, pp.109～110, Gihodo, 1989.6. (in Japanese)
10) Hiroyuki Watanabe, Toshio Suehiro : An experimental study on dynamic earth pressure acting on side walls of underground conduit, Proc. of JSCE, No.432/I-16, pp.155～163, 1991.7. (in Japanese)

(receivede November 25, 1993)

3次元有限要素法による地中構造物と地盤の弾塑性動的応答解析

大嶋義隆・渡辺啓行

地中構造物—地盤連成系模型の振動実験のシミュレーションを3次元有限要素法を用いて行った．地盤および地盤と構造物の接触面の結合要素を塑性流れを考慮した弾塑性体としてモデル化すれば，地盤のダイレタンシー特性によって水平方向加振が上下振動を励起する現象，水平動と上下動による動土圧が構造物に作用する現象の定量的な評価が可能となることを示した．